UNCERTAINTY QUANTIFICATION FOR ATOMISTIC REACTION MODELS: AN EQUATION-FREE STOCHASTIC SIMULATION ALGORITHM EXAMPLE

YU ZOU AND IOANNIS G. KEVREKIDIS *

Abstract.
We describe a computational framework linking Uncertainty Quantification (UQ) methods for continuum problems depending on random parameters with Equation-Free (EF) methods for performing continuum deterministic numerics by acting directly on atomistic/stochastic simulators. Our illustrative example is a heterogeneous catalytic reaction mechanism with an uncertain *atomistic* kinetic parameter; the "inner" dynamic simulator of choice is a Gillespie Stochastic Simulation Algorithm (SSA). We demonstrate UQ computations at the coarse-grained level *in a nonintrusive way*, through the design of brief, appropriately initialized computational experiments with the SSA code. The system is thus observed at three levels: (a) a fine scale for each stochastic simulation at each value of the uncertain parameter; (b) an intermediate coarse-grained state for the *expected behavior* of the SSA at each value of the uncertain parameter; and (c) the desired fully coarse-grained level: distributions of the coarse-grained behavior *over the range of uncertain parameter values*. The latter are computed in the form of generalized Polynomial Chaos (gPC) coefficients in terms of the random parameter. Coarse projective integration and coarse fixed point computation are employed to accelerate the computational evolution of these desired observables, to converge on random stable/unstable steady states, and to perform parametric studies with respect to other (nonrandom) system parameters.

Key words. Uncertainty quantification, Equation-Free, generalized Polynomial Chaos, stochastic Gillespie algorithm, multiscale

1. Introduction. The temporal evolution of many engineering systems can be described through continuum models (typically Ordinary or Partial Differential Equations, ODEs or PDEs) depending on *random* parameters and/or initial/boundary conditions. A number of methods have been proposed to study the evolution of the probability distribution of the solutions of such random problems (the so-called uncertainty quantification or UQ). Among early exploration approaches in this area are Monte-Carlo based methods [1, 2, 3, 4], which normally require a large number of ensemble realizations to achieve convergence. For slightly perturbed systems, whose random parameters can be described as small fluctuations around average values, perturbation methods may be utilized [5, 6, 7]. Such methods cannot, however, be used to treat more generic random systems, exhibiting large parametric uncertainties, and even if used they can only obtain information on low-order statistics. To overcome this difficulty, moment-closure techniques (e.g., [8]) were tried to study dynamics of statistical moments of solutions for which the small-uncertainty assumption in the perturbation method may be relaxed. A significant difficulty with this aprroach lies in deriving an accurate *closure* for high-order statistical moments of the solution distributions; this is extremely difficult, especially for nonlinear systems.

In recent years an alternative approach for UQ, the stochastic Galerkin method, has received considerable attention as an approach to solving ODEs or PDEs with random parameters. This approach originated from the work of Wiener [9] in constructing multiple stochastic integrals (also known as Homogeneous Chaos) to represent functionals of Wiener processes. This idea was then utilized in [10] to express solutions of random systems in terms of Hermite polynomials of Gaussian random

*Department of Chemical Engineering and Program in Applied and Computational Mathematics, Princeton University, Princeton, NJ 08544(yannis@princeton.edu).

variables (i.e., Wiener-Hermite Polynomial Chaos). Projections of these solutions on the Hermite polynomial basis are deterministic, and can be readily numerically solved after truncation through a Galerkin method. Early works in applying the method in engineering systems include [10], where random static and dynamical problems in structural analysis were investigated. The method was subsequently applied in uncertainty quantification of various physical systems including (but certainly not restricted to) porous media [11], fluid dynamics [12] and chemical reactions [13]. The application of the Wiener-Hermite Polynomial Chaos was recently extended in [14, 15, 16] to a general situation, where the Askey scheme was used to construct *generalized* Polynomial Chaos (gPC) with respect to other continuous and discrete probability measures. Other developments in the application of the method include piecewise function representation [17], non-orthogonal expansions [18] and Wiener-Haar wavelet expansions [19]. One advantage of the stochastic Galerkin method relative to Monte Carlo simulation is that it can reduce a random system to a deterministic one, often with considerably fewer degrees of freedom. Moreover, this method – along with its extensions and ramifications – can handle more general uncertainty problems such as large fluctuations, multimodal and discontinuous probability distributions, etc.

In order to implement the stochastic Galerkin method, we must be able to derive differential equations for the projection of solution distributions onto gPC bases (i.e., ODEs for the evolution of gPC coefficients). When explicit equations for these gPC coefficients are not available in closed form, a unified approach, combining equation-free techniques [20, 21, 22] and the stochastic Galerkin method *in a nonintrusive way* has been proposed. This is *equation-free uncertainty quantification* [23], which can evolve gPC coefficients in time, and has been used to perform steady state and limit cycle bifurcation analysis of the gPC coefficient equations without needing these equations in closed form. This approach is based on short bursts of direct simulation (ensembles of such simulations distributed over the random parameter(s)) as an inner, "fine scale" simulator; these bursts are used to numerically estimate the necessary information at the "coarser" gPC coefficient level (e.g., temporal derivatives of gPC coefficients) *on demand*. The main assumption underlying this approach is that the long-term dynamics in gPC coefficient space lie on a low-dimensional, attracting manifold, which can be parametrized by only a few leading-order gPC coeffiicents in the appropriate orthogonal polynomial chaos basis (see [14]). In this way, model reduction can be achieved by using gPC expansions.

When we study continuum models of chemically reacting systems (e.g. ODEs for the evolution of reactant concentrations in a stirred tank reactor, or for the evolution of coverages on catalytic surfaces), UQ techniques can be used to study the effect of uncertainty in kinetic or operating parameters on the overall reactor behavior (e.g. steady state concentrations, reaction rates etc.). In many problems of contemporary interest, however, such continuum differential equations are not available in closed form; instead, we are given a description of the chemical kinetics at an atomistic/stochastic level and the uncertainty enters now in the parameters of the atomistic/stochastic simulation itself (e.g. in certain transition probabilities). The normal steps for uncertainty quantification modeling would involve (a) derivation of closed continuum kinetic equations for the coarse-grained observables of the atomistic simulation (averaged concentrations, averaged coverages)– these equations need to explicitly express *coarse-grained* parameter uncertainty in terms of the *fine scale, atomistic level* parameter uncertainty; and (b) the application of traditional, continuum UQ techniques on these continuum kinetic equations. Here we will show

how to circumvent this "intermediate" derivation of coarse-grained, continuum kinetic equations.

We will implement a computational framework that performs UQ computations for these unavailable, random continuum kinetic equations *by acting on the fine scale, atomistic/stochastic simulator directly*. This uncertainty quantification procedure for stochastic chemical reaction models with uncertain parameters involves three distinct system levels: a fine scale, microscopic simulator *for fixed values of the uncertain parameter(s)*; an *intermediate* coarse-grained scale, where continuum kinetic ODEs exist *in principle* for certain system observables, still for fixed values of the uncertain parameter(s); and, a final, fully coarse-grained scale of gPC coefficients for the distributions of the solutions of these (unavailable) closed form continuum equations. The equation-free machinery is thus used at two successive levels: first to circumvent the derivation of closed form continuum kinetic equations; and then to circumvent the derivation of explicit equations for the evolution of the gPC coefficients for the solutions of these equations with uncertain parameters through a Galerkin procedure.

The paper is organized as follows: We start in Section 2 briefly recalling the formulation of the stochastic Galerkin method. Equation-free techniques are combined with this stochastic Galerkin method in Section 3 to study random systems *without explicitly available governing equations*. The approach is illustrated through the standard model for the $A + 1/2B_2 \rightarrow AB$ reaction, which has been used as a simplified description for the catalytic oxidation of CO [24]. The fine-scale simulator is chosen to be the Gillespie Stochastic Simulation Algorithm (SSA). Computational results are presented in Section 4 where we also demonstrate the efficiency of using the Gauss-Legendre quadrature for computing gPC projections. Random stable/unstable steady-state solutions are also computed in Section 4, and continuation algorithms are implemented to explore the effect of variation of a system (nonrandom) parameter on the statistics of the random steady state. We conclude with a brief summary and discussion in Section 5.

2. The Stochastic Galerkin Method. Consider a system whose evolution in time is governed by the differential equation

$$\frac{d\boldsymbol{x}_c}{dt} = \boldsymbol{f}(\boldsymbol{x}, \omega_c), \quad \boldsymbol{x}_c(\omega_c, 0) = \boldsymbol{x}_{c,0}(\omega_c); \tag{2.1}$$

the system state is $\boldsymbol{x}_c(\omega_c, t)$, where ω_c is an element in the sampling space Ω_c. The subscript c stands for "coarse", since we consider this to be the coarse-grained description of an atomistic simulator (an SSA simulator in our illustrative example below). The solution of the above equation can be described by an expansion in an L^2 space with a generalized polynomial chaos basis $\Psi_i(\boldsymbol{\xi}(\omega_c))$, i.e.,

$$\boldsymbol{x}_c(\omega_c, t) = \sum_{i=0}^{P} \boldsymbol{x}_{cc}^i(t)\Psi_i(\boldsymbol{\xi}(\omega_c)). \tag{2.2}$$

The projections $\boldsymbol{x}_{cc}^i(t)$ are determined by

$$\boldsymbol{x}_{cc}^i(t) = \frac{< \boldsymbol{x}_c(\omega_c, t), \Psi_i(\boldsymbol{\xi}(\omega_c)) >}{< \Psi_i(\boldsymbol{\xi}(\omega_c)), \Psi_i(\boldsymbol{\xi}(\omega_c)) >}, \tag{2.3}$$

where the inner product $< \cdot, \cdot >$ is defined as

$$< q(\boldsymbol{x}(\boldsymbol{\xi})), g(\boldsymbol{x}(\boldsymbol{\xi})) >= \int q(\boldsymbol{x}(\boldsymbol{\xi}))g(\boldsymbol{x}(\boldsymbol{\xi}))p(\boldsymbol{\xi})d\boldsymbol{\xi}, \tag{2.4}$$

(where $p(\boldsymbol{\xi})$ is a probability measure of $\boldsymbol{\xi}$) for any functions $q(\boldsymbol{x}(\boldsymbol{\xi}))$ and $g(\boldsymbol{x}(\boldsymbol{\xi}))$ in the L^2 space. The subscript "cc" is indicative of a second level of coarse-graining: these coefficients describe the *statistics* of the distribution of solutions for the already coarse-grained state $\boldsymbol{x}_c(\omega_c, t)$ over the sampling space.

Through a Galerkin projection, equations governing gPC coefficients $\boldsymbol{x}^i_{cc}(t)$ are obtained as

$$\frac{d\boldsymbol{x}^i_{cc}}{dt} = \frac{< \boldsymbol{f}(\sum_{i=0}^{P} \boldsymbol{x}^i_{cc}(t)\Psi_i(\boldsymbol{\xi})), \Psi_i(\boldsymbol{\xi}) >}{< \Psi_i(\boldsymbol{\xi}), \Psi_i(\boldsymbol{\xi}) >}, \quad i = 0, 2, \cdots, P, \tag{2.5}$$

with $\boldsymbol{x}^i_{cc}(0) = \frac{<\boldsymbol{x}_c(0), \Psi_i(\boldsymbol{\xi})>}{<\Psi_i(\boldsymbol{\xi}), \Psi_i(\boldsymbol{\xi})>}$. The above equation can be formally compactly rewritten as

$$\frac{d\boldsymbol{X}_{cc}}{dt} = \boldsymbol{H}(\boldsymbol{X}_{cc}), \tag{2.6}$$

where

$$\boldsymbol{X}_{cc} = (\boldsymbol{x}^0_{cc}, \boldsymbol{x}^1_{cc}, \cdots, \boldsymbol{x}^P_{cc})^T \tag{2.7}$$

and

$$\boldsymbol{H} = (\boldsymbol{h}_0, \boldsymbol{h}_1, \cdots, \boldsymbol{h}_P)^T. \tag{2.8}$$

Here

$$\boldsymbol{h}_i(\boldsymbol{X}_{cc}) = \frac{< \boldsymbol{f}(\sum_{i=0}^{P} \boldsymbol{x}^i_{cc}(t)\Psi_i(\boldsymbol{\xi})), \Psi_i(\boldsymbol{\xi}) >}{< \Psi_i(\boldsymbol{\xi}), \Psi_i(\boldsymbol{\xi}) >}, \quad i = 0, 2, \cdots, P. \tag{2.9}$$

If $\frac{d\boldsymbol{X}_{cc}}{dt} = \boldsymbol{0}$ in the long-time limit, then Equ.(2.6) has a steady state, which can be used to obtain the probability distribution of the random steady state of (2.1). The explicit derivation of Equation (2.6) is a challenging problem if (2.1) is a set of strongly nonlinear equations; pseudospectral approaches (see e.g. [13]) provide a possible alternative.

3. Equation-Free Computation for Random Dynamical Systems without Explicit Governing Equations. Equation-free methods have been applied in recent years to investigate solutions of *non-random* macroscopic systems whose evolution equations are not explicitly available [20, 24, 21, 22, 25]. The approach can, in principle, provide clear scenarios of the coarse-level evolution and its parametric dependence while requiring only short-time bursts of evolution with the micro-level simulators; in effect, it is a framework of accelerating the extraction of information from the microscale simulation through judicious design of computational experiments and processing of their results.

The equation-free approach utilizes the so-called coarse time-stepper as its basic element; this time-stepper consists essentially of three components: *lifting*, *microsimulation*, and *restriction*. Lifting is a protocol that transforms a coarse-level state to consistent fine-level states; restriction is the converse of lifting. Note that the lifting will, in general, not be a one-to-one transformation, since fine-scale states have far more degrees of freedom than their corresponding coarse-grained descriptions; this is

a vital step in EF computations, and a good code should test, on line, that different realizations of the lifting protocol do not affect the coarse-grained computational results.

This approach was applied recently in conjunction with the stochastic Galerkin method to study random dynamical systems [23]. The fine scale state, in this case, is a (large enough) ensemble of system realizations; at each time snapshot, this ensemble can be represented by its projection onto a generalized polynomial basis; if a low order gPC truncation provides an accurate representation, these first few gPC coefficients constitute the coarse-grained description. In principle, there exist differential equations for these projections, which can be derived, implemented in a computer code, and then solved using numerical methods. However, it may be difficult or even impossible to derive these equations; equation-free methods were utilized as an alternative way of solving them without deriving them first.

Assuming that the coarse-grained evolution is smooth, one can use techniques like projective integration [26, 27] to accelerate the time-evolution of the gPC coefficients using fine scale (ensemble realization) simulations over only relatively short time segments. This is accomplished by *observing* the evolution of the ensemble MC runs on their gPC coefficients (through *restriction*), and use of these data to locally estimate the time-derivative of the coarse-grained description (the local time derivative of the gPC coefficients). This information is then "passed" to traditional continuum numerical initial value problem solvers (ranging from the simple explicit forward Euler to Runge-Kutta type or even implicit integrators) that "project" the coarse-grained state forward in time [21, 22]. One thus solves the initial value problem for the coarse-grained description with the necessary quantities (the gPC local time derivatives) obtained not through a function evaluation from a closed-form model, but through processing the results of "judicious" numerical experiments with the fine scale code. Beyond coarse projective integration, when Equation (2.5) has a stationary state, one can turn the coarse time-stepper into a fixed-point operator and use matrix-free methods such as Newton-GMRES [28] to compute stable/unstable coarse-grained steady states. These correspond to random steady states of the original random equations.

The equation-free technique in [23], however, requires the evolution equations for the random dynamical systems to be explicitly available. In the case that these equations are not explicitly available, we now show how to exploit fine-scale models *underlying* these differential equations. We now have two successive lifting (and, correspondingly, two successive restriction) levels. To obtain a numerical representation for evolution of the desired, "doubly" coarse-grained representation (the gPC coefficients), the fine-scale states of these fine-scale models are first restricted to an intermediate coarse level: we obtain individual states in the ensemble of random ODE solutions. At a second level of restriction, the entire ensemble of these states is used to compute their gPC coeffcients. We view the level of random differential equation as the "intermediate coarse" scale and the level where the gPC projections reside as a desired "fully coarse" scale.

The interaction between intermediate coarse and the fully coarse scale states is embodied in equations (2.2) and (2.3), which correspond to *lifting* and *restriction*, respectively, between these two scales. The interaction between fine and "intermediately coarse" states *at fixed values of the random parameters* $\boldsymbol{\xi}$ is described by two new lifting and restriction mappings: $\boldsymbol{\mu}$ (*lifting*) and $\mathcal{M}$ (*restriction*),

$$\boldsymbol{X}_f(\boldsymbol{\xi}, t) = \boldsymbol{\mu}(\boldsymbol{x}_c(\boldsymbol{\xi}, t)), \tag{3.1}$$

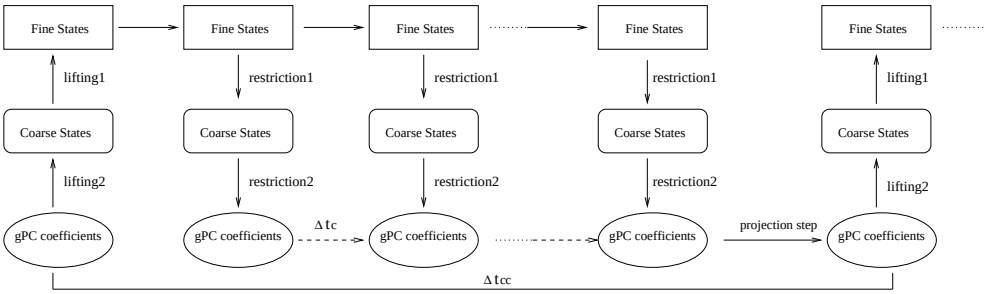

FIG. 3.1. *Schematic of coarse projective integration for multiscale systems with uncertainty.*

$$\boldsymbol{x}_c(\boldsymbol{\xi}, t) = \mathcal{M}(\boldsymbol{X}_f(\boldsymbol{\xi}, t)). \tag{3.2}$$

Recall that the fine-scale states $\boldsymbol{X}_f$ are characterized by many more degrees of freedom than their intermediate-scale $\boldsymbol{x}_c$ counterparts. As the fine-scale states are restricted to the intermediate-scale level, these additional degrees of freedom are eliminated.

Coarse projective integration for random systems whose coarse-scale equations are not explicitly available can be summarized in the following steps: (see Fig. 3.1)

1. Generate an ensemble of (intermediate) coarse-scale states based on initial values of gPC coefficients by (2.2).
2. Generate an ensemble of corresponding fine-scale states consistent with each element of the ensemble of (intermediate) coarse-scale states by (3.1). In the case that (intermediate) coarse-scale states are mean fields, the average of these fine-scale states should be equal to the prescribed (intermediate) coarse state.
3. Evolve fine-scale states via fine-scale (in the example below, SSA) simulators.
4. Restrict the fine-scale states to the (intermediate) coarse level and obtain an ensemble of these coarse-scale states by (3.2).
5. Further restrict (intermediate) coarse-scale states to the desired fully coarse level, to obtain gPC coefficients by (2.3).
6. Perform the above two steps successively, and use the results to estimate the temporal derivative of the fully coarse observables (gPC coefficients). The data collection time is dictated by the separation of fast/slow time scales we assume prevails at the coarse grained level; also by the noise of gPC coefficients brought in by the SSA at the fine level and the approach used to compute these coefficients at the coarse level.
7. *Project forward in time* –using a continuum numerical integrator, such as forward Euler- to obtain the fully coarse observables at a later time. Go back to Step 1. The selection of the projective time step so as to retain overall stability of the projective method is discussed in [26].

In equation-free computations of random coarse-scale steady states, we use the time-stepper for the fully coarse scale states $\boldsymbol{X}_{cc}$ (the gPC coefficients), $\boldsymbol{\Phi}_T$, to construct a fixed point equation

$$\boldsymbol{X}_{cc} = \boldsymbol{\Phi}_T(\boldsymbol{X}_{cc}) \tag{3.3}$$

The operator $\boldsymbol{\Phi}_T$ involves repeated lifting and repeated restriction procedures across two scale gaps, as illustrated in Fig. 3.2. The solution of Equation (3.3) can be attemped either by direction iteration, by Newton's method with numerically estimated Jacobians (for a small number of gPC coefficients) or, more systematically, by

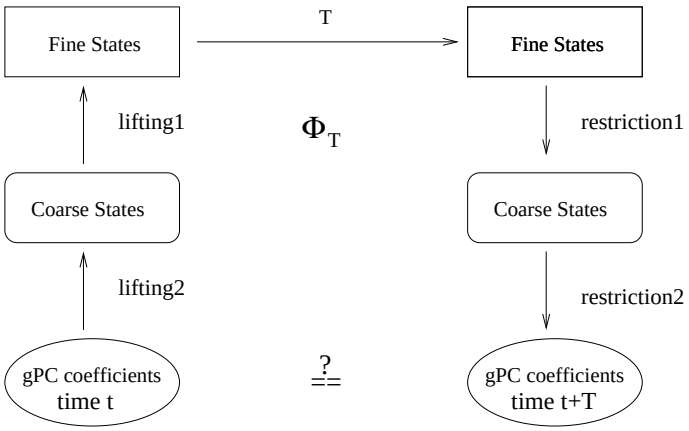

FIG. 3.2. *Fixed-point formulation for coarse random steady states.*

matrix-free fixed point algorithms such as Newton-Krylov GMRES (for large numbers of gPC coefficients) [28]. Once the fully coarse-scale steady states are available, ensemble realizations and thus probability distributions of coarse-scale steady states can be immediately obtained by (2.2).

4. Numerical Results. Our illustrative example involves the $A+1/2B_2 \to AB$ reaction, which can be used as a caricature description of the CO oxidation on a Pt catalyst surface [24]. Our (intermediate) coarse-scale observables are the mean coverages of reactants and the vacant catalyst sites. The fine scale states in each detailed simulation consist of the numbers of sites occupied by each reactant and the vacant sites. In the limit of very large systems, the (intermediate) coarse scale ODEs for mean coverage based on the particular kinetic mechanism would be

$$\begin{aligned} d\theta_A/dt &= \alpha\theta_* - \gamma\theta_A - k_r\theta_A\theta_B \\ d\theta_B/dt &= \beta\theta_*^2 - k_r\theta_A\theta_B \end{aligned} \tag{4.1}$$

(where θ_A, θ_B and θ_* are mean coverages of reactants A, B and vacant sites, respectively). We will not use these equations in our computations that follow (which are performed for *finite size* systems).

At the fine scale description level, there are four elementary reaction steps:

$$\begin{aligned} A(g) + *_i &\xrightarrow{\alpha} A_{*,i} \\ B_2(g) + *_i + *_j &\xrightarrow{\beta} B_{*,i} + B_{*,j} \\ A_{*,i} &\xrightarrow{\gamma} A(g) + *_i \\ A_{*,i} + B_{*,j} &\xrightarrow{k_r} AB(g) + *_i + *_j; \end{aligned} \tag{4.2}$$

here (g) refers to gas phase reactants, $*_{i(j)}$ a vacant site, and $A(B)_{*,i(j)}$ are the absorbed reactants on the surface. At the continuum limit, the rates of four reactions are given respectively by $r_1 = \alpha\theta_* N_{tot}$, $r_2 = \beta\theta_*^2 N_{tot}$, $r_3 = \gamma\theta_A N_{tot}$ and $r_4 = k_r\theta_A\theta_B N_{tot}$, where N_{tot} is the number of sites on the reacting surface. For our finite-size system, the four reaction rates at a given time t (based on which the reaction probabilities are computed) would be $r_1 = \alpha N_*$, $r_2 = \frac{1}{2}\frac{\beta}{N_{tot}} N_*(N_*-1)$, $r_3 = \gamma N_A$ and $r_4 = \frac{k_r}{N_{tot}} N_A N_B$, where N_A, N_B and N_* are numbers of sites taken respectively by A, B and vacant slots at time t.

Our implementations of this chemical reaction scheme follows the Gillespie algorithm [29, 30]. The index of reaction that will take place next depends on the random variable p_1, uniformly distributed over the domain $[0, 1]$: reaction j will occur if $\sum_{i=1}^{j-1} r_i / \sum_{i=1}^{4} r_i \leq p_1 \leq \sum_{i=1}^{j} r_i / \sum_{i=1}^{4} r_i$. The time at which this reaction takes place is $-ln(p_2)/\sum_{i=1}^{4} r_i$, where p_2 is also a uniformly distributed random variable over $[0, 1]$. For each realization in the fine-level SSA, a stoichiometric matrix is then used to keep track of the changes in the numbers of the reactants and vacant sites over time.

In the simulations that follow, the parameters α, γ, and k_r are considered known, and set respectively to 1.6, 0.04 and 4; the uncertain parameter is β: $\beta = 6.0 + 0.25\xi$, where ξ is a random variable uniformly distributed over $[-1, 1]$. Legendre polynomial chaos is chosen as the basis for the random, fully coarse-scale states. The highest truncation order for these fully coarse observables is chosen as 3 ($P = 3$). A total ensemble of 40,000 realizations are used in lifting and restriction between the intermediate coarse (mean coverages) to the fully coarse (gPC coefficients) level. Consistent with each of these 40,000 ensemble realizations, 1000 fine-scale realizations were simulated; each of them uses $200^2 (N_{tot} = 200^2)$ sites on the catalyst surface. The fine-(intermediate) coarse restriction $\mathcal{M}$ consists in taking the average coverage over these 1000 fine-scale realizations corresponding to each (intermediate) coarse observable (i.e., mean coverage of each reactant). We perform successive fine-intermediate coarse and then intermediate-fully coarse restrictions at 40 successive coarse-scale time steps ($\Delta t_c = 0.01s$). We then use least-squares fitting to estimate temporal derivatives of the gPC coefficients based on values at the last 5 time steps. These numerical derivatives are then used (in a simple, forward Euler projective scheme) to calculate gPC states after a relatively large time step ($\Delta t_{cc} = 0.8s$). Figure 4.1 shows evolution of the mean coverage of reactant A as a function of the random variable ξ in the time domain; the "empty" time intervals in the plot are the projective forward Euler "jumps", over which we do not simulate. Figures 4.2 and 4.3 contrast the evolution of the fully coarse-scale observables (gPC coefficients), computed by ensemble average from direct Monte Carlo simulation of the coarse-scale ODEs (4.1), and also computed through projective integration of the two-scale-gap system; Fig. 4.4 compares the standard deviations of mean coverages computed from the gPC coefficients in the two approaches. The results indicate good agreement between projective integration computations and true evolutions at the fully coarse gPC level.

In an attempt to further accelerate the computation, the Gauss-Legendre quadrature was used to approximate the inner product in the intermediate coarse to fully coarse restriction (2.3). In the corresponding fully-to-intermediate coarse lifting, only coarse states corresponding to values of ξ *at the Gauss-Legendre points* were generated. Figures 4.5-4.7 show coarse projective integration results using this method, which utilizes only 200 coarse-scale realizations (rather than 40,000 ones). To display the effectiveness of this technique, we implemented the original Monte-Carlo simulations in the intermediate level by using a total of 200 realizations; the results are shown in figures 4.8 and 4.9. With such a small number of realizations in a Monte Carlo simulation, while the zeroth-order gPC coefficients of mean coverages of reactants are well captured, other, higher order coefficients deviate significantly from their true trajectories even at the beginning of the projective integration. This is clearly due to the lack of sufficient realizations of mean coverage when ensemble averaging is used to compute the corresponding gPC coefficients. Lifting only around Gauss-Legendre quadrature points can enhance the effectiveness of our approach to simulate

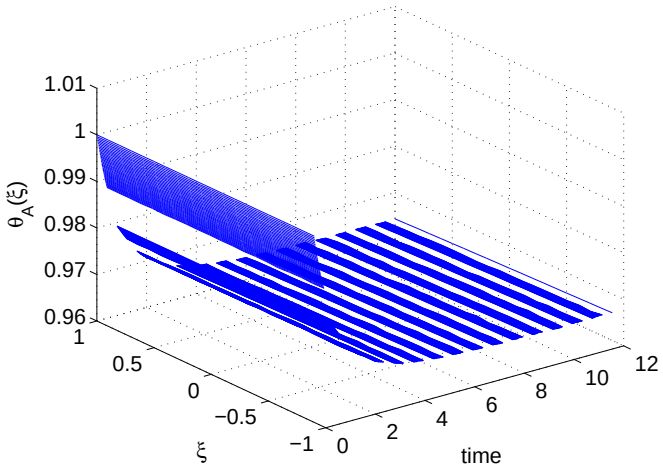

FIG. 4.1. *Evolution of $\theta_{\mathbf{A}}$ as a function of the random variable ξ through coarse projective integration*

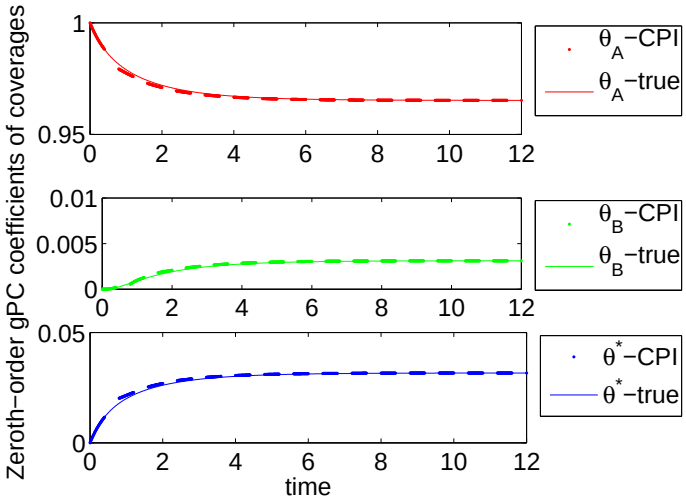

FIG. 4.2. *Evolution of the zeroth-order gPC coefficient of the mean coverages computed by coarse projective integration, with Ne=40,000 randomly selected ξ values; symbols: CPI results; lines: gPC coefficients obtained via Monte Carlo simulation of the coarse ODEs.*

the evolution of gPC coefficients by using a much smaller number of intermediate coarse-level realizations than that required by the standard Monte-Carlo simulation. Computing the gPC coefficient evolution by sampling only close to qudarature points has been proposed (for Gauss-Hermite quadrature, in a problem of approximating PC coefficients for random temperature distribution) in [31].

We also use a matrix-free Newton-Krylov GMRES method to converge on the (deterministic) stable/unstable fully coarse steady states of the gPC coefficient description, out of which random (intermediate) coarse steady state distributions can

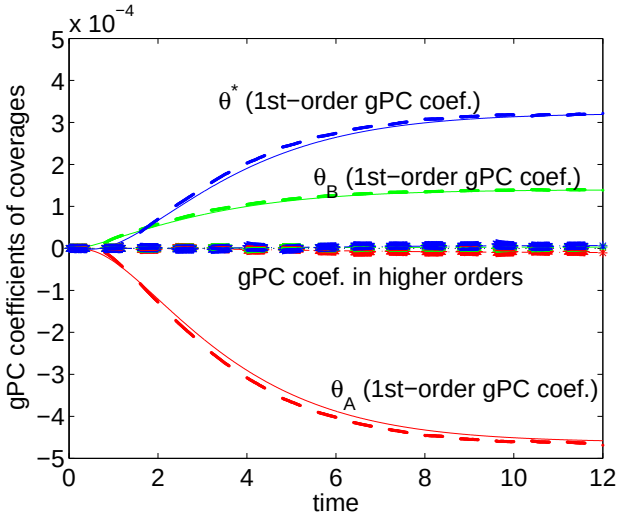

FIG. 4.3. *Evolution of additional (higher-order) gPC coefficients of the mean coverages computed by coarse projective integration with Ne=40,000 randomly selected ξ values; symbols: CPI results; lines: gPC coefficients obtained via Monte Carlo simulation of the coarse ODEs.*

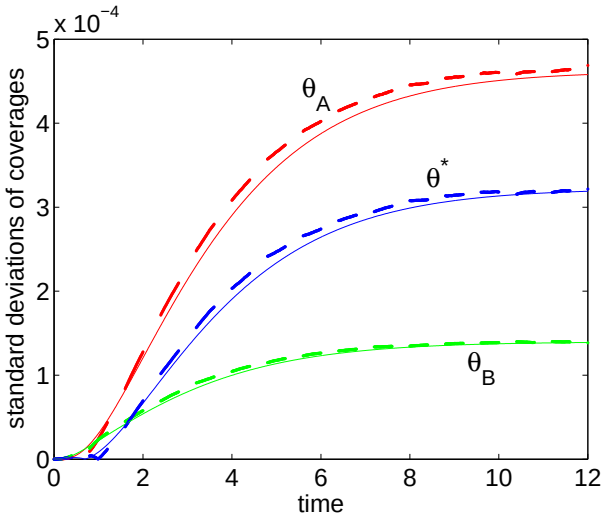

FIG. 4.4. *Evolution of the standard deviations of the mean coverages computed by coarse projective integration, with Ne=40,000 randomly selected ξ values; symbols: CPI results; lines: Monte Carlo simulation of the coarse ODEs.*

be obtained by (2.2). In this computation, $\beta =< \beta > (1.0 + 0.05\xi)$, where ξ is again a uniform random variable in $[-1, 1]$. In Fig. 4.10, dashed lines are true envelopes of random coarse-scale steady states (computed by setting $\beta = 1.05 < \beta >$ and $\beta = 0.95 < \beta >$), and solid lines are the derterministic steady states when $\beta =< \beta >$. Error bars and stars represent respectively ranges and means of random steady states of mean coverages computed using the matrix-free, time-stepper based Newton-Krylov-GMRES method. Clearly, this equation-free fixed-point computation can correctly reproduce the random steady states. Again, values of ξ at

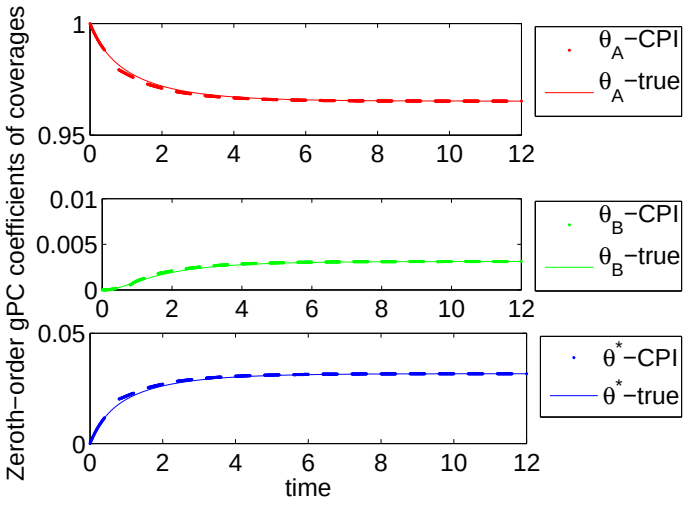

FIG. 4.5. *Evolution of the zeroth-order gPC coefficient of the mean coverages computed by coarse projective integration for Ne=200 ξ values at Gauss-Legendre points; symbols: CPI results; lines: gPC coefficients obtained via Monte Carlo simulation of coarse ODEs.*

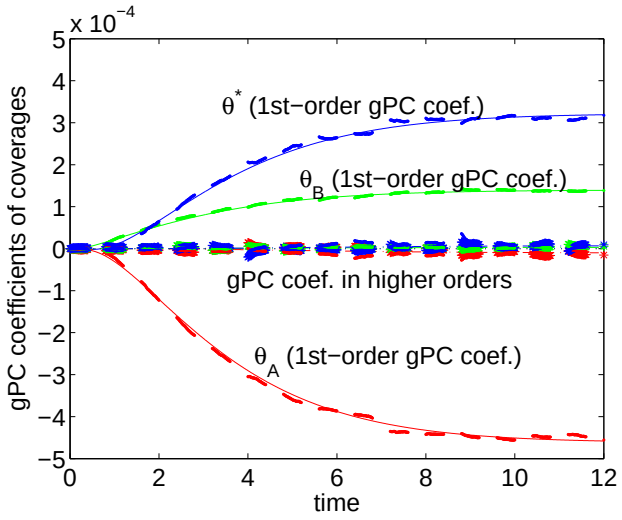

FIG. 4.6. *Evolution of additional (higher-order) gPC coefficients of the mean coverages computed by coarse projective integration with Ne=200 ξ values at Gauss-Legendre points; symbols: CPI results; lines: gPC coefficients obtained via Monte Carlo simulation of the coarse ODEs.*

Gauss-Legendre points are used to generate realizations of intermediately-coarse-scale observables (mean coverages) and implement fixed-point computations (Fig. 4.11). The random steady states can be accurately captured by this technique as well, while the computational load decreases significantly. The approach has been linked with a continuation algorithm to trace the bifurcation diagrams of the random steady states as a function of $< \beta >$; observe that *unstable* random steady states can thus be computed, and bifurcation points (such as turning points of random steady states) in parameter space can be approximated (see Figures 4.10 and 4.11).

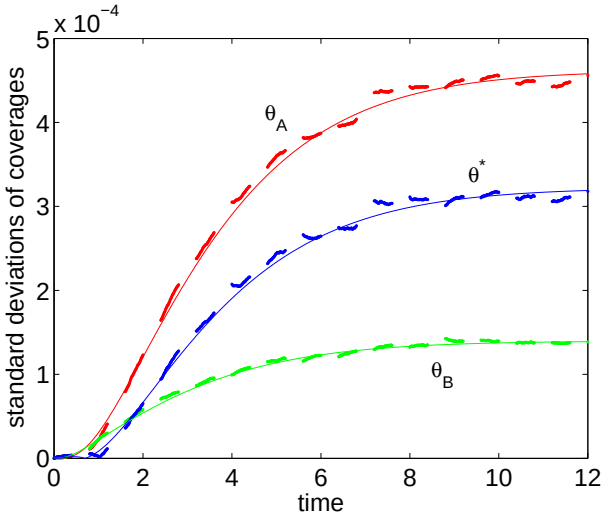

FIG. 4.7. *Evolution of the standard deviations of the mean coverages computed by coarse projective integration with Ne=200 ξ values at Gauss-Legendre points; symbols: CPI results; lines: Monte Carlo simulation of coarse ODEs.*

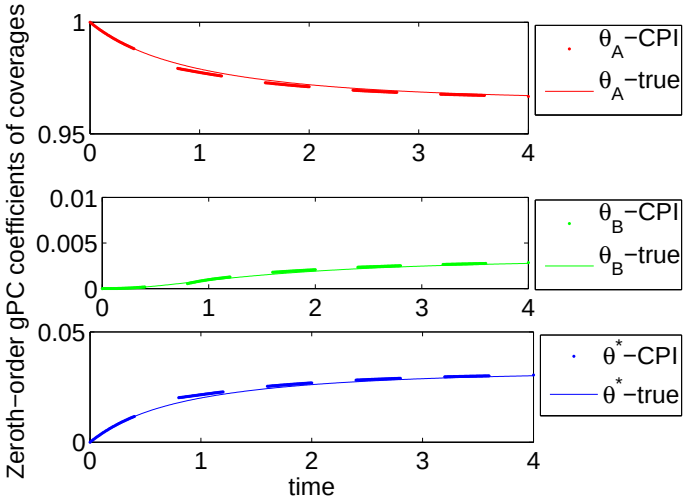

FIG. 4.8. *Evolution of the zeroth-order gPC coefficients of the mean coverages computed by coarse projective integration for Ne=200* randomly selected *ξ values; symbols: CPI results; lines: gPC coefficients obtained via Monte Carlo simulation of coarse ODEs with Ne=40,000.*

5. Summary. Equation-free methods were used at two successive layers, in this paper, to enable uncertainty quantification computations on models of reacting systems for which no coarse-grained, continuum description is available in closed form. Coarse projective integration was used to accelerate the computation of transient dynamics of the problem solution distributions (at gPC coefficients level). Random stable/unstable steady state computation, and their parametric/bifurcation analysis at this gPC coefficient level was also demonstrated. Gauss quadrature rules were used to effectively reduce the computational load while preserving the accuracy of results

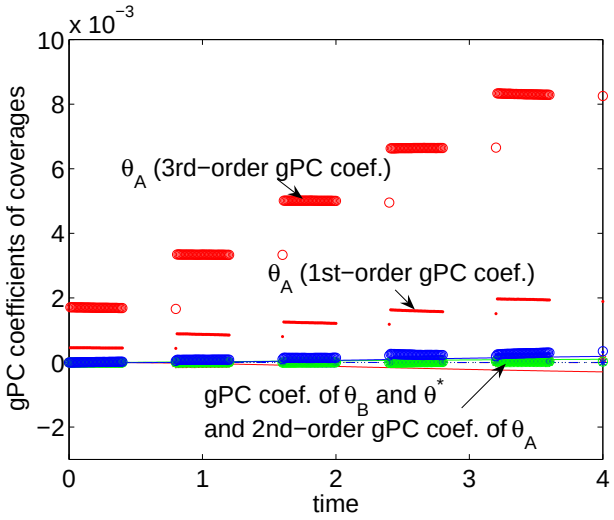

FIG. 4.9. *Evolution of additional, higher-order gPC coefficients of the mean coverages computed by coarse projective integration with Ne=200* randomly selected *ξ values. Red circles and dots represent the 3rd- and 1st-order gPC coefficients of $\theta_{\mathbf{A}}$ obtained by CPI, respectively. Jumps during the course of their evolution are caused by insufficient number of coarse realizations of coverages used to perform ensemble average when computing the gPC coefficiens. Clustered green and blue symbols in the lower part of the figure stand for gPC coefficients of reactant $\theta_{\mathbf{B}}$ and vacancy θ^*, respectively. Lines represent gPC coefficients obtained via Monte Carlo simulation of the coarse ODEs with Ne=40,000. Red, green and blue solid lines stand for respectively the 1st-order gPC coefficients of $\theta_{\mathbf{A}}$, $\theta_{\mathbf{B}}$ and θ^*. Red, green and blue dot-dashed lines stand for respectively the 2nd-order gPC coefficients of $\theta_{\mathbf{A}}$, $\theta_{\mathbf{B}}$ and θ^*. Red, green and blue dotted lines stand for respectively the 3rd-order gPC coefficients of $\theta_{\mathbf{A}}$, $\theta_{\mathbf{B}}$ and θ^*.*

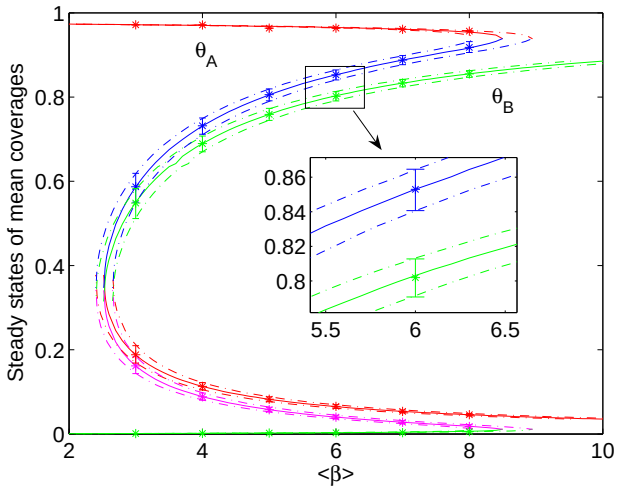

FIG. 4.10. *Bifurcation diagram of the random model steady states with respect to the mean $< \beta >$ of the uncertain parameter distribution. Coarse fixed point computation and continuation with Ne=40,000 randomly selected ξ values; red and green objects: stable steady states; blue and magenta objects: unstable steady states. See text for the inset.*

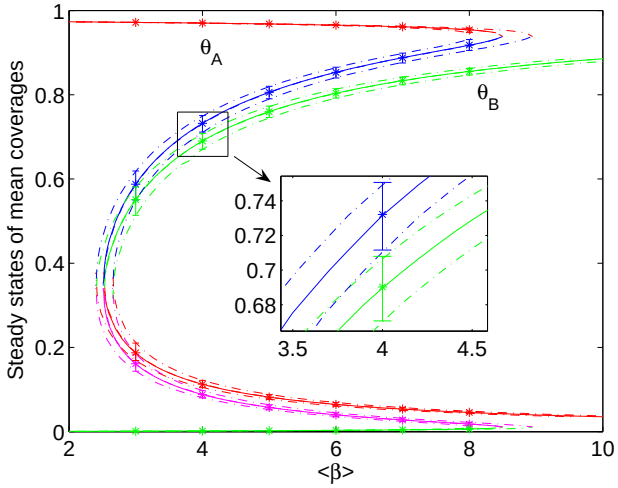

FIG. 4.11. *Bifurcation diagram of the random model steady states with respect to the mean* $< \beta >$ *of the uncertain parameter distribution. Coarse fixed point computation and continuation with Ne=200* ξ *values at Gauss-Legendre points; red and green objects: stable steady states; blue and magenta objects: unstable steady states. See text for the inset.*

of the equation-free results. The method should be applicable in UQ for a wider class of reacting problems, beyond those described through a fine-scale SSA simulator, for which no closed-form kinetic equations are available. We believe that the approach can still serve in cases where we know how to describe uncertainty in the *microscopic* simulation parameters, but we cannot easily translate that in uncertainty descriptions for parameters at the coarse-grained level.

Acknowledgements. This work was partially supported by DARPA and by the US DOE. I.G.K. also acknowledges the support of a 2005 Guggenheim Fellowship.

REFERENCES

[1] N. Metropolis and S. Ulam. The Monte Carlo method. *J. Amer. Stat. Assoc.*, 44:335–341, 1949.
[2] M. Shinozuka. Monte Carlo solution of structural dynamics. *Computers and Structures*, 2:855–874, 1972.
[3] W. Bruns et al. *Monte Carlo applications in polymer science*. Springer-Verlag, 1981.
[4] G.S. Fishman. *Monte Carlo: concepts, algorithms, and applications*. Springer-Verlag, 1996.
[5] E.W Boyce and B.E. Goodwin. Random transverse vibrations of elastic beams. *SIAM Journal*, 12(3):613–629, 1964.
[6] G.C. Hart and J.D. Collins. The treatment of randomness in finite element modeling. *SAE Shock and Vibrations Symposium, Los Angeles, CA*, pages 2509–2519, 1970.
[7] W.K. Liu, T. Belytschko, and A. Mani. Probabilistic finite elements for nonlinear structural dynamics. *Computer Methods in Applied Mechanics and Engineering*, 56:61–81, 1986.
[8] A.T. Bharrucha-Reid (editor). *Probabilistic Methods in Applied Mathematics*. Academic Press, New York, 1968.
[9] N. Wiener. The homogeneous chaos. *Amer. J. Math.*, 60:897–936, 1938.
[10] R.G. Ghanem and P.D. Spanos. *Stochastic Finite Elements: A Spectral Approach*. Springer-Verlag, 1991.
[11] R. Ghanem. Probabilistic characterization of transport in heterogeneous media. *Computer Methods in Applied Mechanics and Engineering*, 158(3-4):199–220, 1998.
[12] O. Le Maitre, O. Knio, M. Reagan, H. Najm, and R. Ghanem. A stochastic projection method

for fluid flow. I: Basic formulation. *J. Comp. Phys.*, 173:481–511, 2001.

[13] M. Reagan, H. Najm, B. Debusschere, O. Le Maitre, O. Knio, and R. Ghanem. Spectral stochastic uncertainty quantification in chemical systems. *Combustion Theory and Modelling*, 8:607–632, 2004.

[14] D.B. Xiu and G.E. Karniadakis. The Wiener-Askey polynomial chaos for stochastic differential equations. *SIAM Journal of Scientific Computing*, 24(2):619–644, 2002.

[15] D.B. Xiu and G.E. Karniadakis. Modeling uncertainty in steady state diffusion problems via generalized polynomial chaos. *Computer Methods in Applied Mathematics and Engineering*, 191:4927–4948, 2002.

[16] D.B. Xiu and G.E. Karniadakis. A new stochastic approach to transient heat conduction modeling with uncertainty. *International Journal of Heat and Mass Transfer*, 46:4681–4693, 2003.

[17] M.K. Deb, I.M. Babuška, and J.T. Oden. Solution of stochastic partial differential equations using Galerkin finite element techniques. *Computer Methods in Applied Mechanics and Engineering*, 190:6359–6372, 2001.

[18] I. Babuška and P. Chatzipantelidis. On solving elliptic stochastic partial differential equations. *Computer Methods in Applied Mechanics and Engineering*, 191(37-38):4093–4122, 2002.

[19] O. Le Maitre, O. Knio, H. Najm, and R. Ghanem. Uncertainty propagation using Wiener-Haar expansions. *Journal of Computational Physics*, 197:28–57, 2004.

[20] K. Theodoropoulos, Y.-H. Qian, and I.G. Kevrekidis. 'Coarse' stability and bifurcation analysis using time-steppers: a reaction diffusion example. *Proc. Natl. Acad. Sci.*, 97(18):9840–9843, 2000.

[21] I.G. Kevrekidis, C.W. Gear, J.M. Hyman, P.G. Kevrekidis, O. Runborg, and K. Theodoropoulos. Equation-free coarse-grained multiscale computation: enabling microscopic simulators to perform system-level tasks. *Comm. Math. Sci.*, 1(4):715–762, 2003.

[22] I.G. Kevrekidis, C.W. Gear, and G. Hummer. Equation-free: the computer-assisted analysis of complex, multiscale systems. *A. I. Ch. Eng. Journal*, 50(7):1346–1354, 2004.

[23] D.B. Xiu, R. Ghanem, and I.G. Kevrekidis. An equation-free approach to uncertain quantification in dynamical systems. *IEEE Computing in Science and Engineering Journal (CiSE)*, 7(3):16–23, 2005.

[24] A.G. Makeev, D. Maroudas, and I.G. Kevrekidis. 'Coarse' stability and bifurcation analysis using stochastic simulators: Kinetic Monte Carlo examples. *Journal of Chemical Physics*, 116:10083–10091, 2002.

[25] Y. Zou, I.G. Kevrekidis, and R. Ghanem. Equation-free dynamic renormalization: self-similarity in multidimensional particle system dynamics. *Physical Review E*, 72:046702, 2005.

[26] C.W. Gear and I.G. Kevrekidis. Projective methods for stiff differential equations. *SIAM Journal of Scientific Computing*, 24(4):1091–1106, 2003.

[27] C.W. Gear and I.G. Kevrekidis. Telescopic projective integrators for stiff differential equations. *Journal of Computational Physics*, 187(1):95–109, 2003.

[28] C.T. Kelley. *Iterative Methods for Linear and Nonlinear Equations*. SIAM, 1995.

[29] D.T. Gillespie. Exact stochastic simulation of coupled chemical reactions. *J. Phys. Chem.*, 81:2340–2361, 1977.

[30] D.T. Gillespie. A rigorous derivation of the chemical master equation. *Physica A*, 188:404–425, 1992.

[31] O. Le Maitre, M. Reagan, H. Najm, R. Ghanem, and O. Knio. A stochastic projection method for fluid flow. II: Random process. *Journal of Computational Physics*, 181:9–44, 2002.